arXiv:2211.13721v1 [cond-mat.mes-hall] 24 Nov 2022

From Hermitian critical to non-Hermitian point-gapped phases

Carlos Ortega-Taberner[1,2] and Maria Hermanns[1,2]

[1] *Department of Physics, Stockholm University, AlbaNova University Center, SE-106 91 Stockholm, Sweden*
[2] *Nordita, KTH Royal Institute of Technology and Stockholm University, SE-106 91 Stockholm, Sweden*

(Dated: November 28, 2022)

Recent years have seen a growing interest in topological phases beyond the standard paradigm of gapped, isolated systems. One recent direction is to explore topological features in non-hermitian systems that are commonly used as effective descriptions of open systems. Another direction explores the fate of topology at critical points, where the bulk gap collapses. One interesting observation is that both systems, though very different, share certain topological features. For instance, both systems can host half-integer quantized winding numbers and have very similar entanglement spectra. Here, we make this similarity explicit by showing the equivalence of topological invariants in critical systems with non-hermitian point-gap phases, in the presence of sublattice symmetry. This correspondence may carry over to other features beyond topological invariants, and may even be helpful to deepen our understanding of non-hermitian systems using our knowledge of critical systems, and vice versa.

I. INTRODUCTION

In recent years non-Hermitian systems have attracted a lot of attention in the condensed-matter community due to the unique phenomena that they can exhibit. In the field of symmetry protected topology, non-Hermitian systems harbor a particularly rich variety of phases, as the non-Hermiticity enhances the ten Hermitian topological classes [1–3] into 38 [4–7]. This enhancement originates in having effectively more symmetries available, as conjugation and transposition are not equivalent any longer. Furthermore, non-Hermiticity may lead to new physics without a Hermitian equivalent: So-called point-gap phases and exceptional points [8, 9] lead to new physics with no Hermitian equivalent, like the skin effect [5, 8, 10–12].

For non-Hermitian systems, we need to distinguish between line-gapped and point-gapped systems. For the former, it is possible to draw a line in the complex plane which separates the different bands. On the other hand, a phase is said to be point-gapped at E_0 if it has a non-zero 'energy vorticity' for this point, i.e. the complex energy bands wind around E_0. While the topology of line-gapped systems can be understood from their connection to Hermitian and anti-Hermitian Hamiltonians [6], point-gapped systems have features that are thought to be intrinsically non-Hermitian. In this paper we will focus on these systems and show how some of their features are inherited from related Hermitian critical models.

The topic of topological phenomena in critical systems has recently been revisited [13–17]. Topology is a global (non-local) property of the system, and it was previously thought that the divergent correlation length of critical systems always rendered the system topologically trivial. However, it has been shown recently that this is not the case [13]. Critical systems can harbor topologically protected zero-energy edge states that are protected by a topological invariant and do not hybridize with the bulk. The topological phases in these systems have been characterized by invariants that are quantized to half-integers [14].

The latter is also true for some non-Hermitian systems. For example, systems in the topological class AI (with a sublattice symmetry S that commutes with time-reversal), are characterized by two winding numbers which can take half-integer values when the system has a point-gap [5, 18–20]. This similarity in the topology of Hermitian critical and non-Hermitian systems has been pointed out in the literature before [21], but to our knowledge it has not yet been explored in depth. In this paper we aim to relate the bulk topological features of critical Hermitian systems and point-gapped non-Hermitian systems. We will introduce two different methods of generalizing a Hermitian critical Hamiltonian to a non-Hermitian one, showing that the resulting model always is in a point-gap phase. We also analyze how bulk topological features evolve with the non-Hermiticity, in particular the topological invariants and the so-called entanglement occupancy spectrum (EOS) [22–24]. While the two generalization considered here are somewhat limited, the second includes two of the most used non-Hermitian models, the Hatano-Nelson model and the SSH chain with unbalanced hopping.

In Hermitian systems the EOS, computed for periodic boundary conditions, provides the same topological information as the surface energy spectrum [25, 26], and it has been connected to topological invariants such as the polarization [27] and the winding number [28]. For non-Hermitian point-gapped systems the bulk-boundary correspondence is broken due to the skin effect. Thus one cannot use the surface spectrum to study bulk topology (and vice-versa). In this case, the EOS becomes more interesting, as it can be computed for periodic boundary conditions and can be related to bulk invariants [29, 30]. Connecting these two, on first glance unrelated types of phases, would allow one to compute objects for non-Hermitian models using Hermitian physics, as well as use the more developed topological classification for non-Hermitian systems to address questions regarding critical

Hermitian systems.

The paper is organized as follows: In section II we cover some necessary background material. In section III, we consider a very simple non-Hermitian generalization to elucidate the main ideas. A more complex generalization is shown in section IV, where the non-Hermiticity is introduced by making the momenta complex. The entanglement occupancy spectrum is discussed in section V. Some explicit examples are covered in Appendix A.

II. BACKGROUND

Throughout the paper, we will restrict the discussion to a general 2-band model given by the Hamiltonian

$$\begin{aligned} H(k) &= \boldsymbol{h}(k)\cdot\sigma \\ &= h_x(k)\sigma_x + h_y(k)\sigma_y \\ &= \begin{pmatrix} 0 & f_1(k) \\ f_2(k) & 0 \end{pmatrix}, \end{aligned} \tag{1}$$

where we set h_z to zero because of sublattice symmetry. Both ways of describing the Hamiltonian will prove useful in the following. Note that for non-Hermitian models, $f_2(k) \neq f_1^*(k)$, while in the Hermitian case we will suppress the index, and use $f(k) \equiv f_1(k) = f_2^*(k)$. The right eigenstates of such two-band Hamiltonians are in general given by

$$v_\pm^R(k) = \frac{1}{\sqrt{2}}(\pm\sqrt{f_1(k)/f_2(k)}, 1) \tag{2}$$

with energies $\pm\sqrt{f_1(k)f_2(k)}$. The corresponding left ones are

$$v_\pm^L(k) = \frac{1}{\sqrt{2}}(\pm\sqrt{f_2(k)/f_1(k)}, 1) \tag{3}$$

For Hermitian two-band models, the winding number [3] can be written as

$$\nu = \frac{1}{2\pi}\int_0^{2\pi} dk\, \partial_k \arg[h_x(k) - ih_y(k)], \tag{4}$$

or alternatively as

$$\nu = \frac{1}{2\pi}\int_0^{2\pi} dk\, \frac{(\partial_k h_x(k))h_y(k) - h_x(k)\partial_k h_y(k)}{h_x(k)^2 + h_y(k)^2}. \tag{5}$$

For non-Hermitian models both expressions are no longer equal. The second expression, Eq. (5), is usually employed to compute the winding number [5, 6, 18]. While the Hamiltonian (1) is, of course, restrictive, it nevertheless covers two of the most studied non-Hermitian models, the Hatano-Nelson model [31–33] and the non-Hermitian extension to the SSH model [34].

A. Topological invariants for critical systems

Topological invariants are usually considered meaningful only in gapped systems. This raises the question if and how topological features survive the presence of gapless modes, e.g. by coupling to a gapless environment [35] or by driving to a phase transition between two topological phases [13, 14]. For the latter, the usual definitions of topological invariants become ill-defined. A general 'recipe' on obtaining well-defined invariants for critical systems was first presented in [14], by removing an infinitesimal region around each of the gapless points.

For the winding number, this implies that instead of (4), we use the following, regularized version:

$$\nu_\epsilon = \frac{1}{2\pi}\int_{()} dk\, \partial_k \arg[h_x(k) - ih_y(k)] \tag{6}$$

where () denotes that we removed a region $[k_c - \epsilon, k_c + \epsilon]$ from the integration around each gapless point k_c. In the limit $\epsilon \to 0$, ν_ϵ becomes half-integer quantized, and is given generically by the mean of the winding numbers on either side of the critical point, for details see Ref. [14]. In particular, at the critical point between gapped phases with winding number 0 and 1 respectively, the winding number $\nu_\epsilon \to 1/2$ for $\epsilon \to 0$.

There is an alternative formulation of the winding number by interpreting $f(= f_1 = f_2^*)$ in Eq. (1) as a complex function, $f(z = e^{ik})$, and relating the winding number to the difference in numbers of zeroes and poles within the unit circle, using Cauchys Theorem [13, 16],

$$\nu = \frac{1}{2\pi i}\oint dz \frac{f'(z)}{f(z)} = Z - P, \tag{7}$$

where Z/P denotes the number of zeroes/poles within the unit circle. This identity is not valid for gapless systems because there is a zero in the contour. One alternative for gapless systems is to again exclude an infinitesimal region around each point z,

$$\nu_\epsilon = \frac{1}{2\pi i}\oint_{()} dz\, \frac{f'(z)}{f(z)}. \tag{8}$$

Each zero of order n on the unit circle contributes $n/2$ to the winding number, in agreement with the discussion in the section above. One could, however, have chosen to define the invariant differently, namely as $\tilde{\nu} = Z - P$, where Z/P are the zeroes and poles strictly within the unit circle. This instead gives an integer (not half-integer) quantized invariant, which in addition is related to the number of topologically protected edge modes [13, 16].

One disadvantage of Verresen's approach in Ref. [14] is that one needs to compute different invariants, depending on whether the system is gapless or gapped — the invariant for gapped systems is ill-defined for gapless ones. A different way of regularizing the winding number for gapless systems was discussed in Ref. [17], namely by

considering the system at finite temperatures. Computing the $T \to 0$ limit in a gapped system yields (4), while doing the same for a critical system yields the $\epsilon \to 0$ limit of Eq. (6), as the Boltzmann weights suppress the contribution in the vicinity of gapless points. It, thus, has the advantage that gapped and gapless systems can be treated on the same footing. The generalization to non-Hermitian systems detailed in sections III and IV can, in some sense, be regarded as yet another regularization of the winding number that treats gapped and gappless systems on the same footing.

Note that the winding number $\lim_{\epsilon\to 0}\nu_\epsilon$ does not uniquely characterize the critical system, nor is it connected to the number of topologically protected edge modes. Two different critical points — e.g. the phase transitions $\nu = 0 \to 3$ and $\nu = 1 \to 2$ — have the same value $\nu = 3/2$ of the winding number. The first critical point has no protected topological egde modes, while the latter has one. In general, the number of topological edge modes is given by [13]

$$N_{\text{top}} = \begin{cases} \tilde{\nu} & \text{if } \tilde{\nu} > 0. \\ |\tilde{\nu} + N| & \text{if } \tilde{\nu} < -N \\ 0 & \text{otherwise} \end{cases}, \tag{9}$$

where $\tilde{\nu} = Z - P = \nu - N/2$, Z/P are the number of zeroes/poles strictly within the unit circle, and N is the number of zeroes (times their multiplicity) on the unit circle. A complete characterization of the critical system thus requires two numbers, e.g. $\tilde{\nu}$ and N. This is very similar to the non-Hermitian, point-gap phases discussed below.

B. Non-Hermitian systems with sublattice symmetry

In this paper, we focus on systems in symmetry class AI, with a sublattice symmetry S that commutes with time-reversal.[36] Such systems are specified by two winding numbers. A commonly used characterization uses winding numbers ν and ν', where ν is given by Eq. (5) and ν' denotes the winding of the complex energy bands around the origin [5, 10] (sometimes referred to as 'energy vorticity'):

$$\nu' = \frac{1}{2\pi}\oint dk\, \partial_k \arg\left(\sqrt{h_x(k)^2 + h_y(k)^2}\right). \tag{10}$$

An alternative formulation was presented in Ref. [18]. Since $f_1 \neq f_2^*$ (1) in non-Hermitian systems, we can define two independent winding numbers by

$$\begin{aligned} \nu_1 &= \frac{1}{2\pi i}\int dk\, \partial_k \ln[f_1(k)] \\ \nu_2 &= -\frac{1}{2\pi i}\int dk\, \partial_k \ln[f_2(k)], \end{aligned} \tag{11}$$

which fulfill

$$\begin{aligned} \nu &= \frac{1}{2}(\nu_1 + \nu_2) \\ \nu' &= \frac{1}{2}(\nu_1 - \nu_2). \end{aligned} \tag{12}$$

Note that the '$-$' sign in the second line of Eq. (11) ensures that $\nu_1 = \nu_2$ in the Hermitian limit. [37] An appealing feature of the winding numbers $\nu_{1/2}$ is that they are directly related to the presence of topologically protected boundary modes present at the right/left edge of a semi-infinite open system [18]. We will later see that $\nu_{1/2}$ also have a natural interpretation in the connected Hermitian, critical system: they can often be identified with the winding numbers of the neighboring gapped phases, which will be discussed in Section IV.

C. Entanglement occupancy spectrum

The entanglement spectrum was originally proposed for strongly interacting fractional quantum Hall liquids [38] as a usefull tool to obtain information about the topology of the state. It is obtained by first partitioning the system into two parts A and B (usually in real space) and tracing out the degrees of freedom in B to obtain the reduced density matrix $\rho_A = \text{Tr}_B(|\psi\rangle\langle\psi|)$, where $|\psi\rangle$ denotes the ground state of the system. We can now define an entanglement Hamiltonian H_A by

$$\rho_A = e^{-H_A}, \tag{13}$$

whose spectrum is called entanglement spectrum and contains valuable information about the topological properties of the system.

The entanglement spectrum is also of interest in non-interacting systems, as it is directly connected to the topological edge modes in gapped topological insulators [25]. Peschel showed that for non-interacting systems one does not need to compute the full many-body entanglement spectrum (a difficult task even for non-interacting systems) [23]. Instead, one can obtain the same information from the spectrum of the reduced correlation matrix

$$C^A_{j,j',\alpha,\beta} = \langle gs|c^\dagger_{j,\alpha}c_{j',\beta}|gs\rangle, \tag{14}$$

where α and β denote internal degrees of freedom, and j, j' denote sites in region A. In the following, we will call the spectrum of C^A the entanglement occupancy spectrum (EOS). Topological states correspond to $\xi = 1/2$ modes of the EOS, since these give rise to degeneracies in the many-body entanglement spectrum. The number of $\xi = 1/2$ modes is identical to the number of topologically protected edge modes, see Ref. [25].

The correlation matrix spectrum for non-Hermitian systems was first studied in Ref. [30]. Since left and right eigenstates are not equivalent any more, there are in principle three distinct versions of Eq. (14), using either the left-left, right-right, or left-right ground states.

As argued in [30], the left-right choice is usually the one that behaves best and which we will use throughout the manuscript. Numerical simulations suggest that the topological features of the EOS for line gap phases are similar to those of hermitian gapped phases. In particular, one finds a one-to-one correspondence between the topological zero-energy states in the open system and the $\xi = 1/2$ modes in the EOS. For a sublattice symmetric model with winding number ν there will be 2ν topological zero energy modes — ν on each edge — and the same number of $1/2$ modes in the EOS.

Focusing on two-band models with sublattice symmetry as in (1), an intuitive way of arguing for this is the following: The correlation matrix in momentum space can be written as

$$C(k) = \frac{1}{2}(\mathbf{1} + Q(k)) \tag{15}$$

where $Q(k)$ is given by

$$Q(k) = \begin{pmatrix} 0 & -\sqrt{f_1(k)/f_2(k)} \\ -\sqrt{f_2(k)/f_1(k)} & 0 \end{pmatrix}, \tag{16}$$

using the explicit form of the left and right eigenvectors in (2) and (3). We can choose the branch cuts of the square root in such a way that $Q(k)$ is continuous and differentiable. In addition, it is 2π periodic in k. Thus, we can interpret Q as a Hamiltonian with sublattice symmetry and compute the winding number relevant for line-gapped systems,

$$\begin{aligned} \nu &= \frac{1}{2\pi i}\int_0^{2\pi} dk\, \partial_k \ln\sqrt{f_1(k)/f_2(k)} \\ &= \frac{1}{2}\frac{1}{2\pi i}\int_0^{2\pi} dk\, \partial_k(\ln f_1(k) - \ln f_2(k)) \\ &= \frac{1}{2}(\nu_1 + \nu_2). \end{aligned} \tag{17}$$

Since the system is line-gapped, $\nu_1 = \nu_2 = \nu$ and $Q(k)$ has the same winding number as the original Hamiltonian. Computing C^A amounts to computing the real space Fourier transform of Q in region A. The latter harbors 2ν topological zero modes, resulting in 2ν $1/2$ modes in the EOS using Eq. (15).

The situation for Hermitian critical and non-Hermitian pointgap phases is more complicated. An imminent problem is that it is not clear which ground state to use in (14). Numerical simulations show that for point-gapped systems, the EOS seems to harbor $\min(N_L, N_R)$ $1/2$ modes, where N_L and N_R are the topological zero modes of a semi-infinite system [39]. In addition, these topological features were seen to be insensitive to the particular choice of ground state, while non-topological modes may be affected. In our numerical simulations, the same seems to hold for critical systems, where now $N_L = N_R$ are the number of topologically protected edge modes on the left/right edge in the open boundary system. We will comment more on this in Section V, where we will also prove the equivalence of the EOS between Hermitian critical and non-Hermitian point-gapped phases for simple, yet non-trivial cases.

III. GENERALIZING EIGENENERGIES

As we mention in the introduction, the aim of this paper is to show the connection in the topological features of critical Hermitian models and point-gapped non-Hermitian ones. In order to do that we first start with Hermitian models at a critical point and deform them to become non-Hermitian, showing that the topological features remain unchanged by this deformation. We will consider two distinct ways of deforming the Hermitian critical system. The first and simpler approach, discussed in this section, amounts to making eigenenergies complex, while keeping the eigenstates unchanged. Since we do not modify the eigenstates, the left and right non-Hermitian eigenstates are still equal to each other and one can use all the usual techniques in Hermitian quantum mechanics. To further simplify the discussion, we will only consider critical systems where the gapless points are zeroes of order 1. Generalizing to higher orders is straightforward. A less restrictive generalization, which also modifies the eigenstates, is discussed in Section IV.

For a given Hermitian Hamiltonian, written in the eigenbasis,

$$H = \sum_{k\mu} \varepsilon_{k\mu} |\psi_{k\mu}\rangle \langle\psi_{k\mu}|, \tag{18}$$

the eigenenergies are modified by adding the following perturbation:

$$\begin{aligned} H(g) &= \sum_{k\mu} \varepsilon_{k\mu}(g) |\psi_{k\mu}\rangle \langle\psi_{k\mu}|, \\ &= \sum_{k\mu} (\varepsilon_{k\mu} + ig\partial_k\varepsilon_{k\mu}) |\psi_{k\mu}\rangle \langle\psi_{k\mu}|, \end{aligned} \tag{19}$$

where $\varepsilon_{k\mu}$ are the energies of the Hermitian system, μ is the band index, and $\partial_k\varepsilon_{k,\mu}$ is by assumption non-zero. By construction, the eigenstates remain intact. As will be shown below, this generalization results in a point-gapped Hamiltonian. However, we first want to illustrate this generalization by the simplest possible example, assuming eigenenergies $\varepsilon_{k,\mu} = \pm\sin(k/2)$ with a single gapless point at $k = 0$. In order to construct the resulting complex bandstructure, it is easier to regard the model as an effective one-band model in an extended Brillouin zone $k \in [-2\pi, 2\pi)$. The resulting complex energies are

$$\tilde{\varepsilon}_k(g) = \sin(k/2) + i\frac{g}{2}\cos(k/2), \tag{20}$$

which is nothing else than the parametric equation of an ellipse in the complex plane. The system has therefore a point-gap around zero. More generally, zeroes of the

hermitian model correspond to crossings of the imaginary axis (with finite imaginary part), while maxima and minima correspond to crossings of the real axis.

In terms of the Hamiltonian (1), the generalization in (19) can be written as

$$\begin{aligned} H(k,g) =&\epsilon(k,g)\hat{h}(k)\cdot\boldsymbol{\sigma} \\ =&[\epsilon(k)+ig\partial_k\epsilon(k)]\hat{h}(k)\cdot\boldsymbol{\sigma} \end{aligned} \tag{21}$$

with both $\epsilon(k)$ and $\hat{h}(k)$ continuous and differentiable. This can always be done for finite-range hopping Hamiltonians. Even though $\hat{h}(k)$ is not uniquely defined at a gapless point k_c, there is a consistent limit

$$\lim_{\delta\to 0}\hat{h}(k_c+\delta)=\lim_{\delta\to 0}\hat{h}(k_c-\delta) \tag{22}$$

as long as $\epsilon(k)$ changes sign at k_c (for a single zero). For explicit examples on how to choose $\epsilon(k)$ and $\hat{h}(k)$, we refer the reader to Appendix A.

We now proceed to compute the winding number ν for the original, critical Hamiltonian, $H(k,0)$, using the conventions of (21). A short calculation shows that ν only depends on $\hat{h}$, but not on ϵ:

$$\begin{aligned} \nu_\epsilon &= \frac{1}{2\pi}\int_{()} dk\,\frac{(\partial_k h_x(k))h_y(k)-h_x(k)\partial_k h_y(k)}{h_x(k)^2+h_y(k)^2} \\ &= \frac{1}{2\pi}\int_{()} dk\,\frac{\epsilon(k)^2\left(\hat{h}'_x\hat{h}_y-\hat{h}_x\hat{h}'_y\right)}{\epsilon(k)^2} \\ &\to \frac{1}{2\pi}\int dk\,\left(\hat{h}'_x\hat{h}_y-\hat{h}_x\hat{h}'_y\right)\quad\text{for }\epsilon\to 0 \end{aligned} \tag{23}$$

where we abbreviated $\partial_k\hat{h}_\alpha=\hat{h}'_\alpha$. The last equality is valid as long as the integrand is regular, i.e. neither $\hat{h}$ or $\hat{h}'$ has singularities at the gapless points of the critical system. This is trivially satisfied for the finite-range hopping models usually considered. The resulting winding number is half-integer quantized, see [14]. Repeating the same computation for the non-hermitian Hamiltonian, we find that the winding number

$$\begin{aligned} \nu(g) &= \frac{1}{2\pi}\int dk\,\frac{(\partial_k h_x(k,g))h_y(k,g)-h_x(k,g)\partial_k h_y(k,g)}{h_x(k,g)^2+h_y(k,g)^2} \\ &= \frac{1}{2\pi}\int dk\,\frac{\epsilon(k,g)^2(\hat{h}'_x\hat{h}_y-\hat{h}_x\hat{h}'_y)}{\epsilon(k,g)^2}, \\ &= \frac{1}{2\pi}\int dk\,\left(\hat{h}'_x\hat{h}_y-\hat{h}_x\hat{h}'_y\right) \end{aligned} \tag{24}$$

is again independent of ϵ (and thus g) and equal to the last line of (23). This shows that the generalization of the critical system to the non-hermitian one does not alter the winding number ν.

We can now continue taking a look at the second non-Hermitian winding number

$$\nu'=\frac{1}{2\pi}\oint_0^{2\pi} dk\,\partial_k\,\mathrm{Im}\log\det[h(k,g)], \tag{25}$$

which is equivalent to the phase winding of one of the energy bands. In order to use the form of Eq. (21), it is advantages to compute $2\nu'$ by extending the integration from 0 to 4π, thus allowing us to consider $\epsilon(k,g)$ as one of the energy bands. In order to compute the winding, we now count the crossings at the positive imaginary axis (with an additional sign depending on the orientation). We will now show that the contribution of all gapless points to the winding number sums up, with only an overall sign depending on the sign of g. Let us fix the sign of g to be positive and focus on one of the gapless points, denoted by k_c. If $\partial_k\epsilon(k)>0$, the crossing happens on the positive imaginary part from $\mathrm{Re}(\epsilon(k_c-\delta))<0$ to $\mathrm{Re}(\epsilon(k_c+\delta))>0$. If instead $\partial_k\epsilon(k)<0$, the crossing happens on the negative imaginary part from $\mathrm{Re}(\epsilon(k_c-\delta))>0$ to $\mathrm{Re}(\epsilon(k_c+\delta))<0$, i.e. it has the same orientation as above. Thus, the contributions of all gapless points simply add up with a positive sign. Switching the sign of g, switches the orientation. Thus, the winding number ν' is given by

$$\nu'=\mathrm{sign(g)N}/2, \tag{26}$$

where the $\frac{1}{2}$ is because our previous argument was made for $2\nu'$. Clearly, ν' itself is not well-defined in the $g\to 0$ limit, though its absolute value is and simply counts the number of gapless points.

IV. GENERALIZATION TO COMPLEX MOMENTUM

So far we have shown a non-Hermitian generalization of critical systems that can be used to relate the topology of both models. However, the generalization considered, modifying only the eigenvalues and not the eigenstates, is overly simplistic and artificial. A more realistic generalization one can make is by performing an analytical continuation of the momenta in the Bloch Hamiltonian into the complex plane, $H(k)\to H(k,g)=H(k-ig)$. For a Hermitian model, a general Bloch Hamiltonian with sublattice symmetry can be written as

$$H(k)=\begin{pmatrix}0 & f\\ f^* & 0\end{pmatrix},\qquad f=\sum_n t_n e^{ikn}, \tag{27}$$

where t_n are all possible hoppings. The non-Hermitian generalization reads

$$H(k,g)=\begin{pmatrix}0 & \sum_n t_n e^{gn}e^{ikn}\\ \sum_n t_n^* e^{-gn}e^{-ikn} & 0\end{pmatrix}. \tag{28}$$

It is equivalent to introducing non-reciprocity in the inter-cell hoping terms, which is one of the most common ways of introducing non-Hermiticity.

Before continuing, let us consider g as a small pertur-

bation,

$$\begin{aligned} H(k,g) =&\boldsymbol{h}(k,g)\cdot\boldsymbol{\sigma} \\ =&h(k,g)\hat{h}(k,g)\cdot\boldsymbol{\sigma} \\ \approx&\Big[h(k)\hat{h}(k)+g(\partial_g h(k,g)|_{g=0})\hat{h}(k) \\ &+gh(k)\partial_g\hat{h}(k,g)|_{g=0}\Big]\cdot\boldsymbol{\sigma}. \end{aligned} \tag{29}$$

Using that $\partial_g \boldsymbol{h}(k,g) = -i\partial_k \boldsymbol{h}(k,g)$,

$$\begin{aligned} H(k,g) \approx&\left[h(k)-ig\partial_k h(k)\right]\hat{h}(k)\cdot\boldsymbol{\sigma} \\ &-igh(k)\partial_k\hat{h}(k)\cdot\boldsymbol{\sigma}, \end{aligned} \tag{30}$$

we note that the first term is exactly the generalization considered in the previous section (up to the unimportant sign of g), but we now obtain a second term that also modifies the eigenvectors. Therefore, in the perturbative limit the two generalizations can be similar, but they are not identical.

In contrast to the first generalization to non-Hermitian systems considered in Section III, it is now much easier to compute the winding numbers $\nu_{1/2}$ and then use their relation to ν and ν' (12) to connect the result to the critical system. We begin by rewriting the expression for winding number ν_1 in (11) in the complex plane, employing $z = e^{ik}$ as the holomorphic variable

$$\nu_1 = \frac{1}{2\pi i}\oint_{|z|=1} dz\,\partial_z \ln[f(ze^{-g})] \tag{31}$$

and using $f(z) = \sum_n t_n z^n$, i.e. the appropriate expression for the critical system.

We can absorb the scale factor by a change of variables, $z' = ze^{-g}$, and obtain

$$\nu_1(g) = \frac{1}{2\pi i}\int_{|z|'=e^{-g}} dz'\,\partial'_z\,\ln[f(z')]. \tag{32}$$

which can now be obtained as $\nu_1 = Z_1 - P_1$, where $Z_1(P_1)$ are the zeros (poles) of $f(z)$ inside the circle $|z| = e^{-g}$ (times their multiplicity). Note that, for the Hamiltonian considered here,

$$\begin{aligned} f(z) =&\sum_{n=-l}^{r} t_n z^n \\ =&\frac{P_{l+r}(z)}{z^l} \end{aligned} \tag{33}$$

is a polynomial with $P = l$ poles at zero and $l + r$ zeros. For most of the commonly used model Hamiltonians, $l = 0$ (e.g. the extension of the SSH model used in Appendix A or the Hatano-Nelson model), but this is by no means a prerequisite.

For ν_2 we perform exactly the same steps, after substituting $k' = -k$ so that f_2 becomes a holomorphic, not anti-holomorphic function after expressing $z = e^{ik'}$:

$$\begin{aligned} \nu_2 =& \frac{1}{2\pi i}\int_0^{2\pi} dk'\,\partial_{k'}\ln f(ze^{g}) \\ =& \frac{1}{2\pi i}\oint_{|z|=1} dz\,\partial_z \ln[f(ze^{g})]. \end{aligned} \tag{34}$$

We can again absorb the scale factor by a change of variables, but now we set $z' = ze^{g}$ instead. Consequently, ν_2 is given by $\nu_2 = Z_2 - P_2$, where $Z_2(P_2)$ are now the zeros (poles) of $f(z)$ inside the circle $|z| = e^{g}$.

For infinitessimal $g > 0$, ν_1 counts (Z-P) for all zeroes/poles that lie strictly within the unit circle, $\nu_1 = \tilde{\nu}$, while ν_2 even counts the zeroes that lie on the unit circle. Assuming we don't go through any phase transition when enlarging g, the difference of the two winding numbers is simply the number of zeros of $f(z)$ on the unit circle times their multiplicity,

$$\begin{aligned} \nu_1(g) - \nu_2(g) =&N \\ =&2\nu'. \end{aligned} \tag{35}$$

When the underlying critical system has only single zeroes, this is consistent with our previous results (26). [40] Interestingly, as long as we look at phase transitions where zeros do not move simultaneously into and out of the unit circle, ν_1, ν_2 also correspond to the winding numbers of the gapped Hermitian phases surrounding the gapless point. However, this interpretation of ν_1, ν_2 depends on our particular generalization from critical to non-Hermitian systems and will not hold in general.

In order to illustrate this, we consider a very small anti-Hermitian perturbation to our Hamiltonian, such that

$$\begin{aligned} f_1(k) &= f(k) + \delta \\ f_2(k) &= f(k) - \delta^*. \end{aligned} \tag{36}$$

Nonzero δ will generically move the complex zeroes either into or out of the unit circle. Let us first consider ν_1, and observe that since $f(z)$ has a zero on the unit circle, we can write $f_1(z)$ as

$$f_1(z) = A(z)(z - z_0) + \delta, \tag{37}$$

where z_0 denotes the position of the gapless point. Given that δ is small, we can approximate $A(z)$ by a constant in the environment of z_0, yielding

$$f_1(z) \approx A(z_0)\,(z - z_0 + \delta/A(z_0)) \tag{38}$$

for $z \approx z_0$. Similarly, for the other winding number we have

$$f_2(z) \approx A(z_0)\,(z - z_0 - \delta^*/A(z_0)) \tag{39}$$

From these expressions we can now deduce how the zeroes move. In the case where δ is real, the zero of one of the functions moves inside the unit circle while the other one moves out, depending on the sign of $\delta * (z_0^* A(z_0)^* + z_0 A(z_0))$. This results in ν_1, ν_2 being the winding numbers of the gapped neighbouring phases of the gapless point. That is no longer the case for purely imaginary δ, as both zeros move in the same direction.

V. ENTANGLEMENT OCCUPANCY SPECTRUM

In this section, we show some rigorous results on the EOS for the non-Hermitian generalizations considered above.

a. EOS for generalizing eigenenergies In this simple case it is trivial to see that the EOS is independent of g, the non-Hermitian parameter. This is because the EOS only depends on the occupied eigenstates, which are not modified by this particular generalization. If we choose to occupy the same eigenstates, independently of g, then the Hermitian and non-Hermitian models will share the same EOS. Furthermore, since the real part of the energies is also independent of g, the common choice of occupying the states with $\mathrm{Re}[\varepsilon_{k\mu}] < 0$ will lead to the same EOS.

When extending the critical model to non-Hermitian phases, we note that $\tilde{\nu}$ in Eq. 9 becomes identical to ν_1 (ν_2) for sufficiently small $g > 0$ ($g < 0$). The second important quanity, the number of gapless points on the unit circle N, is encoded in $|\nu'| = |\nu_1 - \nu_2|/2$. For the non-Hermitian phases that are of current interest, $\nu_{1/2} \geq 0$, which explains their identification with the number of left/right topological edge states in Ref. [18]. However, this identification will fail if one or both of the winding numbers are negative, and one needs to revert to similar arguments as used in Ref. [13] to derive the correct number of topological edge modes. In general, extensive numerical simulations suggest that the number of topological 1/2 states in the EOS is equal to $\min(N_L, N_R)$, where $N_{L/R}$ are the number of edge modes in the semi-infinite chain, see Ref. [39]. In the limit of the Hermitian critical system, this reduces to Eq. (9). Note that even though the second non-Hermitian winding number ν' does not have a well-defined Hermitian limit, its absolute value, $|\nu'| = N/2$, still carries topological information.

b. EOS for generalizing to complex momenta Making the momenta complex, $k \to k - ig$, modifies the eigenenergies in a similar way as for our first generalization (see e.g. (30)), but it will also modify the eigenstates. So it is far from obvious that the EOS will remain qualitatively unchanged by this generalization.

Instead of the correlation matrix P, we will consider the matrix

$$Q = 2P - I, \tag{40}$$

see Eq. (16). The spectrum of the subsystem matrix Q^A is equivalent to the EOS, with the virtual topological states having zero eigenvalue.

For critical systems, the ground state is degenerate and Q generally depends on the particular ground state chosen. For systems with only one gapless point at k_c, there is a well defined procedure to choose the ground state by filling either the + or the − band from (2) for $k \in (k_c, k_c + 2\pi]$. [41] Using this choice of ground state, the momentum space representation of Q becomes

$$Q(k) = \begin{pmatrix} 0 & -e^{i\phi(k)} \\ -e^{-i\phi(k)} & \end{pmatrix}, \tag{41}$$

where $e^{i\phi(k)} = \sqrt{f(k)/f^*(k)}$. Note that $\phi(k)$ is *not* 2π-periodic, in contrast to Hermitian gapped or non-hermitian line-gapped phases, but 4π-periodic, since Eq. (2) implies that $v_+(k + 2\pi) = v_-(k)$. After the non-Hermitian generalization, the Q-matrix becomes

$$Q(k, g) = \begin{pmatrix} 0 & -e^{i\phi(k-ig)} \\ -e^{-i\phi(k-ig)} & \end{pmatrix}. \tag{42}$$

We now assume that ϕ has a special form and can be written as $\exp[i\phi(k)] = \exp(ik\alpha)$. This is, for instance, possible for the critical SSH chain with $\alpha = 1/2$. In this case, the full Q^A matrix is given by

$$\begin{aligned} Q^A_{xy}(g) &= \oint \frac{dk}{2\pi} e^{ik(x-y)} \begin{pmatrix} 0 & e^{i\phi(k-ig)} \\ e^{-i\phi(k-ig)} & \end{pmatrix} \\ &= \oint \frac{dk}{2\pi} e^{ik(x-y)} \begin{pmatrix} 0 & e^{i\alpha k} e^{g\alpha} \\ e^{-i\alpha k} e^{-g\alpha} & \end{pmatrix} \\ &= \oint \frac{dk}{2\pi} e^{ik(x-y)} \begin{pmatrix} e^{g\alpha/2} & 0 \\ 0 & e^{-g\alpha/2} \end{pmatrix} \\ &\quad \times \begin{pmatrix} 0 & e^{i\alpha k} \\ e^{-i\alpha k} & \end{pmatrix} \begin{pmatrix} e^{-g\alpha/2} & 0 \\ 0 & e^{g\alpha}/2 \end{pmatrix} \\ &= U(g) Q^A_{xy}(0) U(g)^{-1}, \end{aligned} \tag{43}$$

where x, y are restricted to lie in A. This is a similarity transformation that leaves the whole spectrum invariant, not just the topological states that one is interested in.

In general, ϕ is not of the special form assumed above and the two spectra will not be equal to each other. Extensive numerical simulations suggest that the 1/2 modes do remain robust, however. Moreover, in models with a finite range, i.e. the ones most commonly used as model systems, we observe only small deviations in the spectra, i.e. they remain *qualitatively* the same. We exemplify in Fig.1, using the critical system defined by $f(k) = 1 + e^{ik} - 2e^{2ik}$, see (1).

Proving the robustness, however, turns out to be difficult. One avenue might be to use the same techniques as in Ref. [28] to construct exact eigenstates of C^A, and link their number to the relevant winding number in the thermodynamic limit. Constructing the form of the C^A eigenstates for both non-Hermitian point-gapped systems and critical systems with only a single gapless point is straightforward. However, this only tells us how eigenstates look if they exist, but not how many of those exist. For the latter, we need to generalize the arguments by [28] to relate their number to the winding number in the thermodynamic limit – a highly non-trivial task.

Another avenue is to construct zero energy eigenstates of Q^A for finite g, using their expression from $g = 0$. This would not prove the correspondence between the number of topological zero-energy edge modes and 1/2 modes of

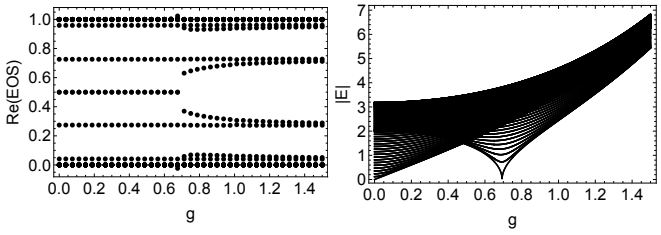


FIG. 1: left: The real part of the EOS as a function of g, when generalizing the critical Hamiltonian defined by $f(k) = 1 + e^{ik} - 2e^{2ik}$, see Eq. (1). The EOS remains qualitiatively unchanged until $g = \ln 2$, where a phase transition to a trivial phase occurs, see right figure.

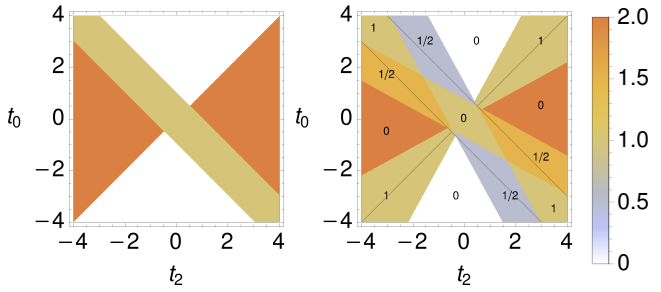


FIG. 2: Phase diagram for Hamiltonian (A1) with $t_1 = 1$ for $g = 0$ (left) and $g = 0.2$ (right). The color code indicates ν, while the numbers indicate ν' (only non-zero for $g \neq 0$).

C^A, but only establish that the topological modes of C^A survive the non-Hermitian generalization. This seems to be more tractable, but is still work in progress.

VI. CONCLUSION

In this manuscript, we have proven analytically that the topological invariants characterizing Hermitian critical systems are the same as those of two distinct generalizations to non-Hermitian point-gap systems. While one of the generalizations also leaves the EOS — a useful tool for characterizing topology — invariant, the other one in general does not. Despite that, numerical simulations strongly suggest that the topological features remain unchanged. We have proven this explicitly for a simple, yet non-trivial model. The close relation between Hermitian critical and non-Hermitian point-gapped phases also lends some physical interpretation to some properties of the latter, in particular explaining the number of topological modes in the EOS.

Our results might be utilized in at least two different ways: we can regard the non-Hermitian generalizations discussed in Sections III and IV as a regularization of the critical phase, which might prove useful in studying critical systems. It also allows us to compute quantities for non-Hermitian models using Hermitian physics and to address questions regarding critical Hermitian systems using the well-studied topological classification for non-Hermitian systems.

During the completion of this manuscript, another work was put forward [42] that deals with the relation of non-Hermitian to Hermitian critical systems. However, in [42] the authors relate Hermitian critical systems to non-Hermitian critical systems. An important aspect of their construction is that the non-Hermitian energy spectrum is real (and gapless). Thus, their construction is distinct from ours, even though many of the features are similar. In particular, also for point-gap phases one obtains an entanglement entropy scaling linear in subsystem size, implying critical behavior.

Acknowledgements— We want to thank Lukas Rødland and Eddy Ardonne for useful discussions. The research in this grant was supported by the Swedish Research Council under grant no. 2017-05162 and the Knut and Alice Wallenberg foundation under grant no. 2017.0157.

Appendix A: Explicit examples

In this section, we want to exemplify some of the statements of the main text. Throughout, we use a simple model Hamiltonian given by

$$\begin{aligned} H &= \boldsymbol{h}(k)\cdot\sigma \qquad \text{with} \\ h_x(k) &= \gamma_0 + \gamma_1\cos(k) + \gamma_2\cos(2k) \\ h_y(k) &= \gamma_1\sin(k) + \gamma_2\sin(2k) \end{aligned} \tag{A1}$$

which implies that

$$f(k) = \gamma_0 + \gamma_1 e^{ik} + \gamma_2 e^{2ik}. \tag{A2}$$

The phase diagram of the hermitian system is shown in 2(a). We will focus our analysis on four critical points given by

$$\begin{aligned} \{\gamma_0,\gamma_1,\gamma_2\} = &\quad (i) \quad \{0,1,-1\} \quad (\nu:\,1\to 2), \\ = &\quad (ii) \quad \{-1,1,0\} \quad (\nu:\,0\to 1), \\ = &\quad (iii) \quad \{-1,1,-1\} \quad (\nu:\,0\to 2), \\ = &\quad (iv) \quad \{-\frac{1}{2},1,-\frac{1}{2}\} \quad \text{(tricritical)}. \end{aligned} \tag{A3}$$

Without loss of generality we assume $g > 0$ in the following.

a. Generalizing eigenenergies Let us first consider the first method, described in Section III, on how to connect these critical points to non-Hermitian point-gap phases. Below, we give the analytical expressions for $\epsilon(k,g)$ as well as $\hat{h}$.

(i) $\nu : 1 \to 2$:

$$\begin{aligned} \epsilon(k,g) &= 2\sin(k/2) + ig\cos(k/2) \\ \hat{h}_x(k) &= \sin[(3k)/2] \\ \hat{h}_y(k) &= \cos[(3k)/2] \end{aligned} \tag{A4}$$

(ii) $\nu : 0 \to 1$:

$$\begin{aligned}\epsilon(k,g) &= 2\sin(k/2) + ig\cos(k/2)\\ \hat{h}_x(k) &= -\sin(k/2),\\ \hat{h}_y(k) &= -\cos(k/2)\end{aligned} \tag{A5}$$

(iii) $\nu : 0 \to 2$:

$$\begin{aligned}\epsilon(k,g) &= 1 - 2\cos(k) + 2ig\sin(k)\\ \hat{h}_x(k) &= \cos(k),\\ \hat{h}_y(k) &= -\sin(k)\end{aligned} \tag{A6}$$

(iv) tricritical:

$$\begin{aligned}\epsilon(k,g) &= 1 - \cos(k) + ig\sin(k)\\ \hat{h}_x(k) &= \cos(k)\\ \hat{h}_y(k) &= -\sin(k)\end{aligned} \tag{A7}$$

Note first that whenever there are an odd number of gapless points, $\epsilon(k)$ cannot be chosen as 2π periodic, but must be 4π periodic. This is intimately related to $\hat{h}(k+2\pi) = -\hat{h}(k)$ and, thus, a half-integer quantized winding number. The winding numbers of (i) and (ii) are $3/2$ and $1/2$ respectively. For case (iii) and (iv), we note that both ϵ and $\hat{h}$ are 2π-periodic. The corresponding winding number is 1. On first glance, it may be suprising that the winding number of the tricritical point is at all well-defined. It is, however, a fact that appears again in our second non-Hermitian generalization. In the latter, the tricritical point connects to the same point-gapped phase as (iii).

b. Generalizing to complex momenta We now consider the non-Hermitian generalization of critical systems, obtained by letting the momenta become complex as $e^{ik} \to e^{ik-g}$. The resulting phase diagram is shown in Fig. 2, with the color code indicating ν and the numbers indicating ν'. Note that increasing g turns the critical line into point-gap phases, while gapped phases smoothly evolve to line-gapped phases (with $\nu' = 0$) as expected [6].

For (i) $\nu : 1 \to 2$ and using $z = e^{ik}$, f_1 is given by

$$f_1(z) = e^{-g}z - e^{-2g}z^2 = e^{-g}z(1 - e^{-g}z), \tag{A8}$$

which has single zeroes at $z = 0$ and $z = e^{ig}$. Thus, the second zero has moved outside the unit circle and the resulting winding number in Eq. (31) evaluates to 1. For f_2 we instead find

$$f_2(z) = e^{g}z - e^{2g}z^2 = e^{g}z(1 - e^{g}z) \tag{A9}$$

with $z = e^{ik'} = e^{-ik}$, which has single zeros at $z = 0$ and $z = e^{-ig}$. Thus the zero has moved inside the unit circle and the resulting winding number, see Eq.(34), is 2.

For case (ii), f_1/f_2 instead become

$$f_{1/2} = -1 + ze^{\mp g}, \tag{A10}$$

which when compared to (i) above lacks the single zero at $z = 0$, thus yielding $\nu_1 = 0$ and $\nu_2 = 1$ when evaluating the winding number integrals.

For case (iii),

$$\begin{aligned}f_{1/2} &= -1 + ze^{\mp g} - z^2 e^{\mp 2g}\\ &= \left(z - e^{-\pi i/3}e^{\mp g}\right)\left(z - e^{i\pi/3}e^{\mp g}\right),\end{aligned} \tag{A11}$$

thus both zeroes move simultaneously either inside or outside the unit circle yielding $\nu_1 = 0$ and $\nu_2 = 2$.

Last but not least, for case (iv) one finds

$$\begin{aligned}f_{1/2} &= -\frac{1}{2} + ze^{\mp g} - \frac{1}{2}z^2 e^{\mp 2g}\\ &= \left(z - e^{\mp g}\right)^2,\end{aligned} \tag{A12}$$

which is completely equivalent to case (iii), except that both zeroes now sit at the same point. Again, the winding numbers are given by $\nu_1 = 0$ and $\nu_2 = 2$. In all these cases, the gapless point(s) for each winding number move either all inside or all outside, thus allowing us to identify ν_1 and ν_2 with the gapped phases on each side of the critical point.

[1] A. Altland and M. R. Zirnbauer, Nonstandard symmetry classes in mesoscopic normal-superconducting hybrid structures, Physical Review B **55**, 1142 (1997).

[2] A. P. Schnyder, S. Ryu, A. Furusaki, and A. W. W. Ludwig, Classification of topological insulators and superconductors in three spatial dimensions, Physical Review B **78**, 195125 (2008).

[3] A. W. W. Ludwig, Topological phases: Classification of topological insulators and superconductors of non-interacting fermions, and beyond, Physica Scripta **T168**, 014001 (2015).

[4] D. Bernard and A. LeClair, A classification of non-hermitian random matrices, in *Statistical Field Theories* (Springer Netherlands, Dordrecht, 2002) pp. 207–214.

[5] Z. Gong, Y. Ashida, K. Kawabata, K. Takasan, S. Higashikawa, and M. Ueda, Topological phases of non-hermitian systems, Physical Review X **8**, 031079 (2018).

[6] K. Kawabata, K. Shiozaki, M. Ueda, and M. Sato, Symmetry and topology in non-hermitian physics, Physical Review X **9**, 041015 (2019).

[7] H. Zhou and J. Y. Lee, Periodic table for topological bands with non-Hermitian symmetries, Physical Review B **99**, 235112 (2019).

[8] E. J. Bergholtz, J. C. Budich, and F. K. Kunst, Exceptional topology of non-Hermitian systems, Reviews of Modern Physics **93**, 015005 (2021).

[9] Y. Ashida, Z. Gong, and M. Ueda, Non-hermitian physics, Advances in Physics **69**, 249 (2020).

[10] N. Okuma, K. Kawabata, K. Shiozaki, and M. Sato, Topological Origin of Non-Hermitian Skin Effects, Physical Review Letters **124**, 086801 (2020).

[11] N. Okuma and M. Sato, Quantum anomaly, non-Hermitian skin effects, and entanglement entropy in open systems, Physical Review B **103**, 085428 (2021).

[12] E. Edvardsson and E. Ardonne, Sensitivity of non-Hermitian systems, Physical Review B **106**, 115107 (2022).

[13] R. Verresen, N. G. Jones, and F. Pollmann, Topology and edge modes in quantum critical chains, Physical Review Letters **120**, 057001 (2018).

[14] R. Verresen, Topology and edge states survive quantum criticality between topological insulators (2020), arXiv:2003.05453 [cond-mat.str-el].

[15] R. Verresen, R. Thorngren, N. G. Jones, and F. Pollmann, Gapless topological phases and symmetry-enriched quantum criticality, Physical Review X **11**, 041059 (2021).

[16] O. Balabanov, D. Erkensten, and H. Johannesson, Topology of critical chiral phases: Multiband insulators and superconductors, Physical Review Research **3**, 043048 (2021).

[17] O. Balabanov, C. Ortega-Taberner, and M. Hermanns, Quantization of topological indices in critical chains at low temperatures, Physical Review B **106**, 10.1103/physrevb.106.045116 (2022).

[18] C. Yin, H. Jiang, L. Li, R. Lü, and S. Chen, Geometrical meaning of winding number and its characterization of topological phases in one-dimensional chiral non-Hermitian systems, Physical Review A: Atomic, Molecular, and Optical Physics **97**, 052115 (2018).

[19] H. Jiang, C. Yang, and S. Chen, Topological invariants and phase diagrams for one-dimensional two-band non-Hermitian systems without chiral symmetry, Physical Review A: Atomic, Molecular, and Optical Physics **98**, 052116 (2018).

[20] S. Masuda and M. Nakamura, Relationship between the Electronic Polarization and the Winding Number in Non-Hermitian Systems, Journal of the Physical Society of Japan **91**, 043701 (2022).

[21] S. Sarkar, Quantization of geometric phase with integer and fractional topological characterization in a quantum Ising chain with long-range interaction, Scientific Reports **8**, 5864 (2018).

[22] I. Peschel, M. Kaulke, and Ö. Legeza, Density-matrix spectra for integrable models, Annalen der Physik **8**, 153 (1999).

[23] I. Peschel, LETTER TO THE EDITOR: Calculation of reduced density matrices from correlation functions, Journal of Physics A Mathematical General **36**, L205 (2003), arXiv:cond-mat/0212631.

[24] I. Peschel and V. Eisler, The conceptual background of density-matrix renormalization, in *Computational Many-Particle Physics*, edited by H. Fehske, R. Schneider, and A. Weiße (Springer Berlin Heidelberg, Berlin, Heidelberg, 2008) pp. 581–596.

[25] L. Fidkowski, Entanglement spectrum of topological insulators and superconductors, Physical Review Letters **104**, 130502 (2010).

[26] H. Yao and X.-L. Qi, Entanglement entropy and entanglement spectrum of the Kitaev model, Physical Review Letters **105**, 080501 (2010).

[27] C. Ortega-Taberner and M. Hermanns, Relation of the entanglement spectrum to the bulk polarization, Physical Review B **103**, 195132 (2021).

[28] K. Monkman and J. Sirker, Entanglement properties of one-dimensional chiral topological insulators 10.48550/ARXIV.2207.10558 (2022).

[29] L. Herviou, J. H. Bardarson, and N. Regnault, Defining a bulk-edge correspondence for non-Hermitian Hamiltonians via singular-value decomposition, Physical Review A **99**, 052118 (2019).

[30] L. Herviou, N. Regnault, and J. H. Bardarson, Entanglement spectrum and symmetries in non-Hermitian fermionic non-interacting models, SciPost Physics **7**, 069 (2019).

[31] N. Hatano and D. R. Nelson, Localization Transitions in Non-Hermitian Quantum Mechanics, Physical Review Letters **77**, 570 (1996).

[32] N. Hatano and D. R. Nelson, Vortex pinning and non-Hermitian quantum mechanics, Physical Review B **56**, 8651 (1997).

[33] N. Hatano and D. R. Nelson, Non-Hermitian delocalization and eigenfunctions, Physical Review B **58**, 8384 (1998).

[34] S. Yao and Z. Wang, Edge States and Topological Invariants of Non-Hermitian Systems, Physical Review Letters **121**, 086803 (2018).

[35] P. Bonderson and C. Nayak, Quasi-topological phases of matter and topological protection, Physical Review B **87**, 195451 (2013).

[36] In the notation of Table VII in reference [6] we consider systems in AI with S_+.

[37] We should note that our conventions differ from those of [18]. Using a tilde to indicate the conventions of the latter, we use $\nu = -\tilde{\nu}$, $\nu' = \tilde{\nu}'$, $\nu_1 = -\tilde{\nu}_2$ and $\nu_2 = -\tilde{\nu}_1$.

[38] H. Li and F. D. M. Haldane, Entanglement spectrum as a generalization of entanglement entropy: Identification of topological order in non-abelian fractional quantum hall effect states, Physical Review Letters **101**, 010504 (2008).

[39] C. Ortega-Taberner, L. Rødland, and M. Hermanns, Polarization and entanglement spectrum in non-hermitian systems, Phys. Rev. B **105**, 075103 (2022).

[40] In case the critical system has zeroes with higher multiplicity, the two generalizations to non-hermitian systems are *not* equivalent, as (26) only depends on the number of zeroes, but not their multiplicity. This is a direct consequence of the generalization in Section III being too simplistic.

[41] This choice ensures that the Resta polarization behaves consistent with the $T \to 0$ limit of finite-temperature computations [17].

[42] C.-T. Hsieh and P.-Y. Chang, Relating non-Hermitian and Hermitian quantum systems at criticality https://doi.org/10.48550/arXiv.2211.12525.